



Original Article

# <sup>125</sup>I Radioactive Particles Drive Protective Autophagy in Hepatocellular Carcinoma by Upregulating ATG9B

Yunhua Xiao<sup>1</sup>, Jing Yuan<sup>2</sup>, Chongshuang Yang<sup>1</sup>, Junru Xiong<sup>1</sup>, Liangyu Deng<sup>1</sup>, Qinghua Liang<sup>1</sup>, Chuang He<sup>1</sup>, Liangshan Li<sup>1</sup>, Fengtian He<sup>3\*</sup>  and Xuequan Huang<sup>1\*</sup> 

<sup>1</sup>Department of Nuclear Medicine, the First Affiliated Hospital of Army Medical University, Army Medical University, Chongqing, China; <sup>2</sup>Department of Radiology, Army Medical Center, Chongqing, China; <sup>3</sup>Department of Biochemistry and Molecular Biology, College of Basic Medical Sciences, Army Medical University, Chongqing, China

Received: 13 January 2022 | Revised: 27 April 2022 | Accepted: 10 May 2022 | Published: 6 June 2022

## Abstract

**Background and Aims:** <sup>125</sup>I radioactive particles implantation have demonstrated efficacy in eradicating hepatocellular carcinoma (HCC). However, progressive resistance of HCC to <sup>125</sup>I radioactive particles has limited its wide clinical application. **Methods:** We investigated the cellular responses to <sup>125</sup>I radioactive particles treatment and autophagy-related 9B (ATG9B) silencing in HCC cell lines and Hep3B xenografted tumor model using Cell Counting Kit-8 reagent, western blotting, immunofluorescence, flow cytometry, transmission electron microscopy and immunohistochemistry. **Results:** In this study, we demonstrated that <sup>125</sup>I radioactive particles induced cell apoptosis and protective autophagy of HCC *in vitro* and *in vivo*. Inhibition of autophagy enhanced the radiosensitivity of HCC to <sup>125</sup>I radioactive particles. Moreover, <sup>125</sup>I radioactive particles induced autophagy by upregulating ATG9B, with increased expression level of LC3B and decreased expression level of p62. Furthermore, ATG9B silencing downregulated LC3B expression and upregulated p62 expression and enhanced radiosensitivity of HCC to <sup>125</sup>I radioactive particles *in vitro* and *in vivo*. **Conclusions:** Inhibition of ATG9B enhanced the antitumor effects of <sup>125</sup>I particle radiation against HCC *in vitro* and *in vivo*. Our findings suggest that <sup>125</sup>I particle radiation plus chloroquine or/and the ATG9B inhibitor may be a novel therapeutic strategy for HCC.

**Citation of this article:** Xiao Y, Yuan J, Yang C, Xiong J, Deng L, Liang Q, et al. <sup>125</sup>I Radioactive Particles Drive Protective Autophagy in Hepatocellular Carcinoma by Upregulating

ATG9B. J Clin Transl Hepatol 2023;11(2):360–368. doi: 10.14218/JCTH.2022.00023.

## Introduction

Hepatocellular carcinoma (HCC) is the fifth most commonly diagnosed malignancy, and the incidence rate continues to steadily increase.<sup>1</sup> In China, the mortality rate of HCC ranks fifth among all cancers, and approximately 55% patients are diagnosed at stage III or IV.<sup>2</sup> Transarterial chemoembolization (TACE) is considered as the first-line treatment for patients with advanced HCC.<sup>3</sup> However, most advanced HCC patients experience tumor recurrence after TACE partly because nondense deposition of iodized oil results in incomplete occlusion of tumor supply vessels.<sup>4</sup> In addition, the current interventional technology is limited. Treatment of liver cancer located at the hilar region and gallbladder is an urgent clinical problem to be solved. Recent research has shown that brachytherapy with iodine-125 (<sup>125</sup>I) particle implantation effectively controlled the progression of residual HCC in complex regions such as the hilar region and gallbladder for advanced HCC patients after TACE, which had good clinical therapeutic effectiveness that provided a rationale for the application of brachytherapy in advanced HCC patients.<sup>4,5</sup> <sup>125</sup>I radioactive particles continuously radiate  $\gamma$ -rays at 29 keV, causing damage to double-stranded DNA and inducing HCC cell death.<sup>4,6–9</sup> However, some HCC tumors are resistant to <sup>125</sup>I particle radiation,<sup>10</sup> which limits its therapeutic efficacy. Therefore, better understanding of the mechanism underlying the radioresistance of HCC to <sup>125</sup>I particle radiation is required.

Autophagy is an evolutionarily conserved programmed degradation mechanism by which long-lived, damaged, or toxic proteins, and organelles are engulfed and digested in response to environmental stress.<sup>11,12</sup> Autophagy has two distinct cellular functions, including protective autophagy and autophagic cell death.<sup>10,13–15</sup> In addition, autophagy can prevent tumor initiation, proliferation, invasion, and metastasis, especially in the early stage of tumors. It can also promote tumor cell survival and resistance to chemoradiotherapy in the medium-term and advanced stages of tumors.<sup>16</sup> A recent study indicated that <sup>125</sup>I particle radiation mediated autophagy to facilitate cell survival at an early stage.<sup>6</sup> Another report found that <sup>125</sup>I particle radia-

**Keywords:** <sup>125</sup>I radioactive particles; Hepatocellular carcinoma; Autophagy; ATG9B.

**Abbreviations:** ATG9B, autophagy-related 9B; CQ, chloroquine; GAPDH, glyceraldehyde 3-phosphate dehydrogenase; HCC, hepatocellular carcinoma; <sup>125</sup>I, iodine-125; IHC, immunohistochemical; qRT-PCR, real-time quantitative reverse-transcription polymerase chain reaction; shRNA, short hairpin RNA; TACE, transarterial chemoembolization; TEM, transmission electron microscopy; TUNEL, terminal deoxynucleotidyl transferase dUTP nick end labeling.

**\*Correspondence to:** Fengtian He, Department of Biochemistry and Molecular Biology, College of Basic Medical Sciences, Army Medical University, No. 30 Gaotanyan, Shapingba, Chongqing 400038, China. ORCID: <https://orcid.org/0000-0002-1689-6281>. Tel: +86-23-68771348, Fax: +86-23-68752262, E-mail: <mailto:hefengtian66@163.com>; Xuequan Huang, Department of Nuclear Medicine, the First Affiliated Hospital of Army Medical University, Army Medical University, No.30 Gaotanyan, Shapingba, Chongqing 400038, China. ORCID: <https://orcid.org/0000-0002-0807-5563>. Tel: +86-13629774403, Fax: +86-23-68765018, E-mail: [huangxq68@tmmu.edu.cn](mailto:huangxq68@tmmu.edu.cn)

tion triggers autophagy by upregulating the level of reactive oxygen species (ROS) to promote cellular homeostasis and survival in colorectal cancer.<sup>17</sup> <sup>125</sup>I particle radiation-induced autophagic flux by increasing the production of ROS, and autophagy inhibition by 3-methyladenine enhanced the radiosensitivity of esophageal squamous cell carcinoma.<sup>18</sup> These findings suggest that <sup>125</sup>I particle radiation-induced autophagy may also play a role in the resistance of HCC to radiotherapy. However, the association between <sup>125</sup>I particle radiation and autophagy in HCC has not yet been studied, to the best of our knowledge.

In this study, we found that <sup>125</sup>I particle radiation promoted HCC cell death and mediated autophagy *in vitro* and *in vivo*. We also found that inhibition of autophagy by chloroquine diphosphate (CQ) facilitated HCC cell death *in vitro* and *in vivo*, suggesting that <sup>125</sup>I particle radiation-mediated autophagy enhanced HCC cell survival. Moreover, <sup>125</sup>I particle radiation-mediated autophagy by upregulating ATG9B expression, and silencing ATG9B in the presence of <sup>125</sup>I particle radiation promoted radiation sensitivity of HCC. Our findings suggest that ATG9B was involved in the promotion of radiation resistance of HCC by <sup>125</sup>I particle radiation-mediated protective autophagy.

## Methods

### Cell culture

Huh7 and Hep3B human HCC cells, were purchased from the Guangzhou Cellcook Biotech Co., Ltd (Guangzhou, China) and Cell Bank of Type Culture Collection of Chinese Academy of Sciences (Shanghai, China). The HCC cells were cultured in RPMI 1640 medium (Hyclone Laboratories, GE Healthcare Life Sciences, Chicago, IL, USA) supplemented with 10% fetal bovine serum (Gibco, Thermo Fisher Scientific, Inc., Waltham, MA, USA) and 100 U/mL penicillin/streptomycin (Hyclone) in a humidified 5% CO<sub>2</sub> atmosphere at 37°C.

### Short hairpin (sh)RNA transfection

ATG9B shRNAs were purchased from Sigma-Aldrich (St. Louis, MO, USA), and the shRNA sequences are shown as follow: shRNA1 sense: 5'-CCGGCATCCAGAACCTGGACAGTTTCTCGAGAAACTGTCCAGGTTCTGGAT-GTTTTT-3', shRNA1 antisense: 5'-CCGGGCATCCTGCGCTACACCAACTCG-AGTTGGGTAGCGCAGGATGCTTTTTT-3'; shRNA2 sense: 5'-CCGG-CTT-TGCCCTTATGGATGTGAACCTCGAGTTCCACATCCATAAGGGCAA-GTTTTT-3', shRNA2 antisense: 5'-CCGGCGAGTACAACAA-GATGCAGCTCTCGAGA-GCTGCATCTTGTGTACTCGTTTTT-3'. Cells were seeded in 12-well culture plates for 24 h prior to transfection with shRNAs using Lipofectamine 2000 reagent (Invitrogen, Thermo Fisher Scientific, Inc., Waltham, MA, USA) according to the manufacturer's instructions. At 48 h post-transfection, ATG9B expression was assayed, and the transfected cells were used for subsequent experiments.

### Radiation source and irradiation procedure

<sup>125</sup>I radioactive particles (apparent activity 0.8 mCi/seed, mode 6711) were supplied by Beijing Zhibo Bio-Medical Technology Co, Ltd (Beijing, China). <sup>125</sup>I radioactive particles emit 27.4–31.5 keV X rays and 35.5 keV gamma rays, and the half-life of each seed is 59.4 days. We constructed an *in vitro* direct irradiation model as described in previous studies.<sup>7</sup> Briefly, 16 <sup>125</sup>I radioactive particles were equally

spaced around the circumstance at a radius of 17.5 mm and eight particles at a radius of 8.75 mm. Cells were seeded in a 35 mm polystyrene cell culture dishes and cultured for receiving the initial radiation dose rate of 2.7 cGy/h. To deliver cumulative radiation doses of 2, 4, 6, and 8 Gy, cells were exposed for 26, 52, 79, and 106 h, respectively.

### Cell viability and proliferation assays

Cell viability was assayed using Cell Counting Kit-8 reagent (CCK-8; Nanjing KeyGen Biotech Co., Ltd., Nanjing, China). Briefly, cells were seeded into 96-well plates at 100 cells per well. After overnight growth, cells were treated with or without Chloroquine diphosphate (CQ) (Sigma-Aldrich) for 7 days. The culture medium was replaced with 100 μL RPMI 1,640 supplemented with 10 μL CCK-8 reagent and the cells were incubated for 1 h at 37°C. The absorbance of each well was measured at a wavelength of 450 nm.

### Western blotting

Cell lysates (30 μg) were separated by sodium dodecyl sulfate-polyacrylamide gel electrophoresis and transferred to polyvinylidene fluoride membranes. After blocking, the membranes were incubated with primary antibodies against LC3B (#12741; Cell Signaling Technology, Danvers, MA, USA), p62 (#23214; Cell Signaling Technology), and ATG9B (ab240897; Sigma-Aldrich) overnight at 4°C followed by incubation with secondary antibodies (Invitrogen) for 1 h at room temperature. The antibody-antigen complexes were visualized by an electrochemiluminescence substrate kit (Tiangen Biotech Co., Ltd., Beijing, China).

### Apoptosis assay

Cells were harvested immediately after irradiation and double stained with propidium iodide (Keygen Biotech) and Annexin V-EGFP for 20 m at room temperature. The samples were then assayed using flow cytometry (CytoFLEX; Beckman Coulter Inc., Brea, CA, USA).

### Immunofluorescence

Cells were fixed in ice cold methanol for 5 m and then washed with phosphate-buffered saline (PBS) three times. After blocking with 5% bovine serum albumin for 1 h at room temperature, the cells were then incubated with primary antibodies against LC3B (#12741; Cell Signaling Technology, USA) overnight at 4°C followed by incubation with Alexa Fluor 488-conjugated secondary antibody (Invitrogen) for 1 h at room temperature. After washing three times, the nuclei were stained with 4',6-diamidino-2-phenylindole (DAPI) for 10 m. The stained cells were observed with a fluorescence microscope (LSM880; Zeiss, Oberkochen, Germany).

### Transmission electron microscopy (TEM)

Cell culture preparations were fixed in 2.5% glutaraldehyde phosphate buffer overnight at 4°C, washed with PBS and postfixated with 1% osmium tetroxide for 2 h at 4°C. After dehydration in a graded ethanol series, the cells were embedded in Epoxy EMBED-812 resin (Electron Microscopy Sciences, Hatfield, PA, USA), followed by polymerizing for 48

h at 60. Ultrathin sections were stained with lead citrate and uranyl acetate. The sections were then examined and photographed with a transmission electron microscope (H-7650; Hitachi Ltd., Tokyo, Japan).

### Animal assays

BALB/c nude mice (BALB/c-nu/nu, 4–5 weeks of age) were obtained from GemPharmatech Co., Ltd (Chengdu, China). Equal numbers of Hep3B cells ( $5 \times 10^6$ ) were subcutaneously injected into the left axilla of the mice and tumor growth was monitored. Tumor volumes  $v = (\text{length} \times \text{width}^2) / 2$  was recorded every 3 days. When the average tumor volume reached 300–350 mm<sup>3</sup>, the mice were randomly separated into four groups ( $n = 5$  mice/group): (1) PBS controls; (2) CQ; (3) <sup>125</sup>I particle implantation + PBS; and (4) <sup>125</sup>I particle implantation + CQ. <sup>125</sup>I particles (0.8 mCi) were implanted into the center of each tumor mass using an 18 g needle. CQ (50 mg/kg, 0.1 mL) or PBS (0.1 mL) was administered intraperitoneally every other day. The cumulative radiation dose for each mouse was approximately 20 Gy at the end of the treatment after 2 weeks. All nude mice were then euthanized and tumors were excised and processed for histopathological examination. All animal experiments were conducted in accordance with the guidelines of animal care and were reviewed and approved by the ethics committee of the First Affiliated Hospital of Army Medical University (No. AMUWEC20200407).

### Histopathological examination

Histopathological examination was performed with 5 μm deparaffinized tissue sections. Immunohistochemical (IHC) staining was performed following standard protocols. The sections were incubated with primary antibodies against LC3B (#12741; Cell Signaling Technology), p62 (#23214; Cell Signaling Technology), and ATG9B (ab240897; Sigma-Aldrich) after blocking endogenous peroxidase activity and antigen retrieval. Terminal deoxynucleotidyl transferase dUTP nick end labeling (TUNEL) assays were performed to assess cell apoptosis using *In Situ* Cell Death Detection kits (Roche Diagnostics GmbH, Mannheim, Germany) following the manufacturer's instructions. The number of TUNEL-positive cells and relative integrated optical density were quantified using Image Pro Plus 6.0 software (Media Cybernetics Inc., Bethesda, MD, USA). At least five randomly chosen high-power ( $\times 400$ ) fields were evaluated in each tissue section. The investigator who evaluated the slides and analyzed the data was blinded to the animal experiment procedure.

### RNA sequencing and real-time quantitative reverse-transcription polymerase chain reaction (qRT-PCR) assays

Total RNA was extracted using TRIzol Reagent (15596018; Invitrogen). The quantification, qualification, library preparation, and subsequent Sequencing of RNA samples was conducted by Novogene Co., Ltd (Beijing, China). Differential expression analysis of the two conditions was performed using the edge R package (version 3.18.1). *P*-values were adjusted using the Benjamini-Hochberg method. An adjusted *p*-value of 0.05 and an absolute fold-change of two were set as thresholds of significant differential expression. We verified the sequencing results of the key molecules related to this study using qRT-PCR and western blotting assays. Glyceraldehyde 3-phosphate dehydrogenase (GAPDH)

mRNA internal controls of gene expression. The primers for ATG9B are as follows: F, 5'-GCCAACCAACCAAGTACCATAC; R, 5'-AGTAGCTGAAGAGGTTGCAGACT.

### Statistical analysis

Statistical analysis was performed using SPSS version 23.0 (IBM Corp., Armonk, NY, USA). Graphs were drawn with GraphPad Prism 6.0 (GraphPad Software, Inc., La Jolla, CA, USA). All data were reported as means  $\pm$  SDs. Student's *t* test was used to compare the means of two samples of normally distributed data. Analysis of variance followed by Tukey's test was used for multiple comparisons. *P*-values < 0.05 was considered statistically significant.

### Results

#### <sup>125</sup>I particle radiation promotes HCC cell death and induces autophagy *in vitro* and *in vivo*

We investigated the effect of <sup>125</sup>I particle radiation on HCC cell survival using two HCC cell lines, Huh7 and Hep3B. Treatment of cells with <sup>125</sup>I particles with 6 Gy for 3 days resulted in 50% inhibition of cell growth *in vitro* (Fig. 1A, B). Therefore, 6 Gy for 3 days was selected as the standard procedure of <sup>125</sup>I particle radiation in subsequent experiments. To determine whether <sup>125</sup>I particle radiation-induced autophagy of HCC cells, we examined the expression of two markers of autophagy, LC3B and p62. We found that <sup>125</sup>I particle radiation significantly increased the expression of LC3B and decreased the expression of p62 *in vitro* (Fig. 1C). We also observed an increased number of autophagosomes in HCC cells treated with <sup>125</sup>I particle radiation (Fig. 1D, E).

To evaluate the role of <sup>125</sup>I particle radiation on tumor growth *in vivo*, we constructed a xenograft mouse model in which HCC cells were injected into subcutaneous tissues of mice. <sup>125</sup>I particles were implanted into the tumors 2 weeks after they had formed. We found that <sup>125</sup>I particle radiation significantly reduced tumor volume and weight (Fig. 1F–H). We further observed increased expression of LC3B and decreased expression level of p62 in the xenografts, as well as increased numbers of autophagosomes (Supplementary Fig. 1A). Together, the results suggested that <sup>125</sup>I particle radiation caused HCC cell death and mediated autophagy of HCC cells *in vitro* and *in vivo*.

#### <sup>125</sup>I particle radiation induces protective autophagy of HCC cells *in vitro* and *in vivo*

To determine the role of <sup>125</sup>I particle radiation-mediated autophagy in HCC cell survival, we used CQ, an inhibitor of autophagy. We found that CQ significantly promoted <sup>125</sup>I particle radiation-mediated HCC cell apoptosis *in vitro* (Fig. 2A, B, Supplementary Fig. 2A, B). Furthermore, CQ significantly rescued <sup>125</sup>I particle radiation-mediated increased expression of LC3B and decreased expression level of p62 (Fig. 2C, D, Supplementary Fig. 2C).

To evaluate whether inhibition of autophagy enhanced the effect of <sup>125</sup>I particle radiation on suppressing tumor growth *in vivo*, we treated mice with CQ after <sup>125</sup>I particles were implanted into tumors. CQ plus <sup>125</sup>I particle radiation significantly decreased tumor size and weight compared with the changes observed with <sup>125</sup>I particle radiation alone (Fig. 2E–G). Together, the results suggested that <sup>125</sup>I particle radiation-induced protective autophagy to promote the

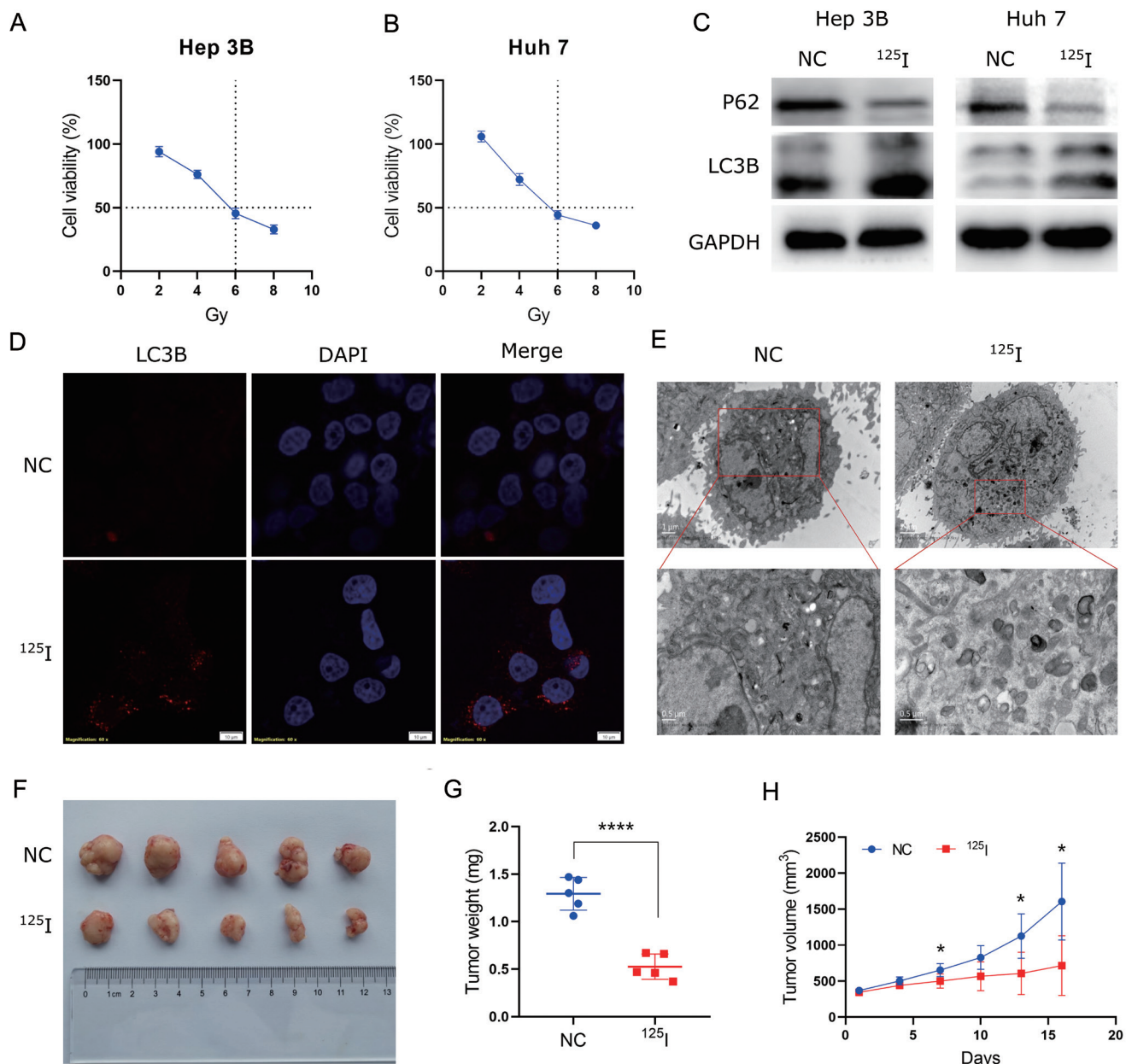


**Fig. 1.** <sup>125</sup>I particle radiation promotes HCC cell death and induces autophagy *in vitro* and *in vivo*. (A and B) Cell viability of Hep3B and Huh7 cells at different times after <sup>125</sup>I particle radiation. (C) Western blot analysis of p62 and LC3B in Hep3B and Huh7 cells treated with <sup>125</sup>I particle radiation for 72 h. GAPDH served as the internal reference. (D and E) Immunofluorescence and TEM presents autophagosomes in Hep3B cells treated with <sup>125</sup>I particle radiation for 72 h. (F) Representative images of tumors from Hep3B cells. <sup>125</sup>I particles were injected into xenografts when the average tumor volume was approximately 300 mm<sup>3</sup>. (G) Tumor weight (mg) of the collected tumor mass removed from mice xenografted with Hep3B cells. (H) Tumor volumes are means±SD. \**p*<0.05, \*\*\*\**p*<0.0001. HCC, hepatocellular carcinoma; TEM, transmission electron microscope.

radioresistance of HCC.

***<sup>125</sup>I particle radiation induces autophagy by increasing the expression level of ATG9B in vitro***

To investigate the underlying mechanism of <sup>125</sup>I particle radiation-mediated protective autophagy in HCC, we performed RNA sequencing in the xenograft tumor tissues with or without <sup>125</sup>I particle radiation. The results identified 592 upregu-

lated mRNAs and 211 downregulated mRNAs (Fig. 3A). Gene Ontology term analysis showed that the dysregulated genes were associated with autophagosome membrane (Supplementary Fig. 3A). Clustering histogram revealed that *ATG9B* was the most significantly upregulated gene (Fig. 3B). *ATG9B* is an upstream molecule in the progression of autophagy,<sup>40</sup> and the result is in line with the observation that <sup>125</sup>I particle radiation-induced autophagy might occur via increased expression of *ATG9B*. We confirmed that <sup>125</sup>I particle radiation significantly increased the expression of *ATG9B* mRNA and protein in HCC cells (Fig. 3C, D).

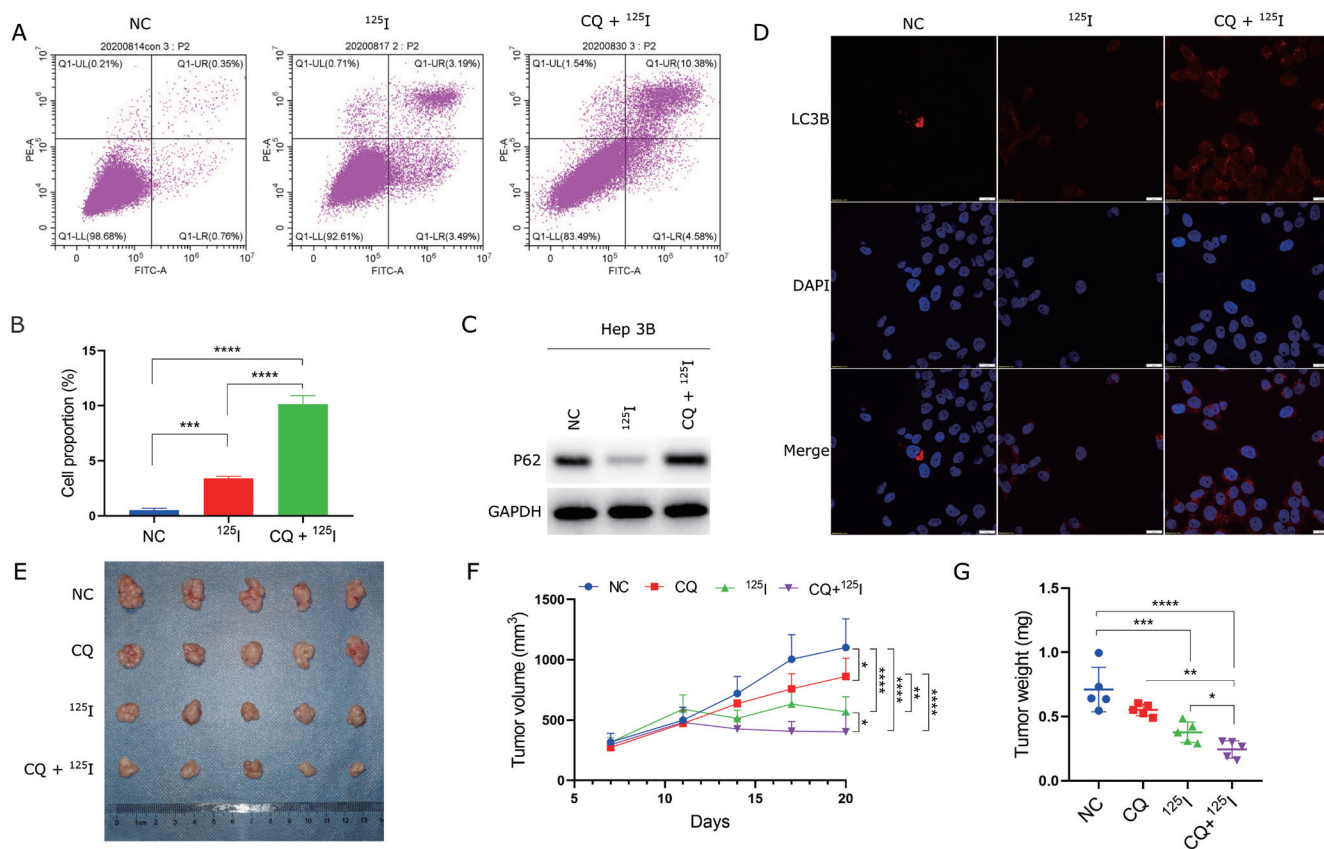


**Fig. 2.** <sup>125</sup>I particle radiation induces protective autophagy of HCC cells *in vitro* and *in vivo*. (A and B) Hep3B cell apoptosis was analyzed using flow cytometry analysis of Annexin V and PI staining. The cells were treated by <sup>125</sup>I particles or cotreated with <sup>125</sup>I particles and CQ for 72 h. (C) Western blot analysis of p62 protein expression in Hep3B cells. The cells were treated by <sup>125</sup>I particles or cotreated with <sup>125</sup>I particles and CQ for 72 h. GAPDH served as the internal reference. (D) Immunofluorescence assay showed that CQ reversed the upregulated expression of LC3B induced by <sup>125</sup>I particles in Hep3B cells (200×). (E) Representative images of tumors at 20 days after inoculation using Hep3B cells treated with CQ or <sup>125</sup>I particle radiation. <sup>125</sup>I particles were injected into xenografts when the average tumor volume achieved approximately 300 mm<sup>3</sup> and CQ was used at the same time. (F–G) Tumor volumes and tumor in the treatment groups are shown. \**p*<0.05, \*\**p*<0.01, \*\*\**p*<0.0001, \*\*\*\**p*<0.0001. HCC, hepatocellular carcinoma; <sup>125</sup>I, iodine-125; CQ, chloroquine; GAPDH, glyceraldehyde 3-phosphate dehydrogenase.

To further determine whether ATG9B was involved in protective autophagy induced by <sup>125</sup>I particle radiation, we performed stable knockdown of ATG9B in HCC cells using lentiviral-mediated ATG9B shRNAs. The results confirmed that ATG9B shRNA-expressing lentivirus resulted in significantly decreased expression of ATG9B mRNA and protein (Supplementary Fig. 3B, D). We found that ATG9B knockdown suppressed ATG9B protein level in HCC cells in the presence of <sup>125</sup>I particle radiation (Fig. 4A, B and Supplementary Fig. 4A, B) and inhibited the proliferation of HCC cells (Fig. 4C, D and Supplementary Fig. 4C, D) compared with controls. Moreover, silencing of ATG9B significantly decreased the expression of LC3B and increased the expression of p62 in HCC cells (Fig. 4E, F and Supplementary Fig. 4E, F). The results suggested that <sup>125</sup>I particle radiation-induced protective autophagy of HCC cells by upregulating ATG9B.

#### **<sup>125</sup>I particle radiation induces autophagy by increasing ATG9B *in vivo***

To further evaluate whether <sup>125</sup>I particle radiation-induced protective autophagy by regulating ATG9B *in vivo*, we used HCC cells silenced for ATG9B to construct a mouse model. We found that silencing ATG9B significantly decreased tu-

mor size and weight in the presence of <sup>125</sup>I particle radiation (Fig. 5A–C). Silencing of ATG9B also significantly decreased LC3B expression and increased p62 expression with <sup>125</sup>I particle radiation in the xenograft tissues (Fig. 5D, E). Furthermore, silencing ATG9B significantly promoted HCC cell apoptosis with <sup>125</sup>I particle radiation as determined by TUNEL assays in the xenograft tissues (Fig. 5F, G). The results suggested that <sup>125</sup>I particle radiation-induced protective autophagy via upregulating ATG9B *in vivo*.

#### **Discussion**

<sup>125</sup>I particle implantation, is a new, local radiotherapy, that is widely used clinically and is a safe, effective, and economical therapeutic strategy in various malignancies, including prostate, head and neck, pancreatic, and lung cancer.<sup>19–22</sup> Importantly, the effect of iodine-125 is not restricted by tumor size, portal vein tumor thrombus, or the heat sink effect of surrounding vessels. This approach also represents a new prospect for HCC treatment.<sup>4</sup> Previous studies confirmed that advanced HCC patients achieved good therapeutic results in response to <sup>125</sup>I particle implantation treatment. However, some patients were not sensitive to the treatment, which has limited its use.<sup>4,5,23–25</sup> The adverse effects caused by <sup>125</sup>I particle radiation are mainly associated

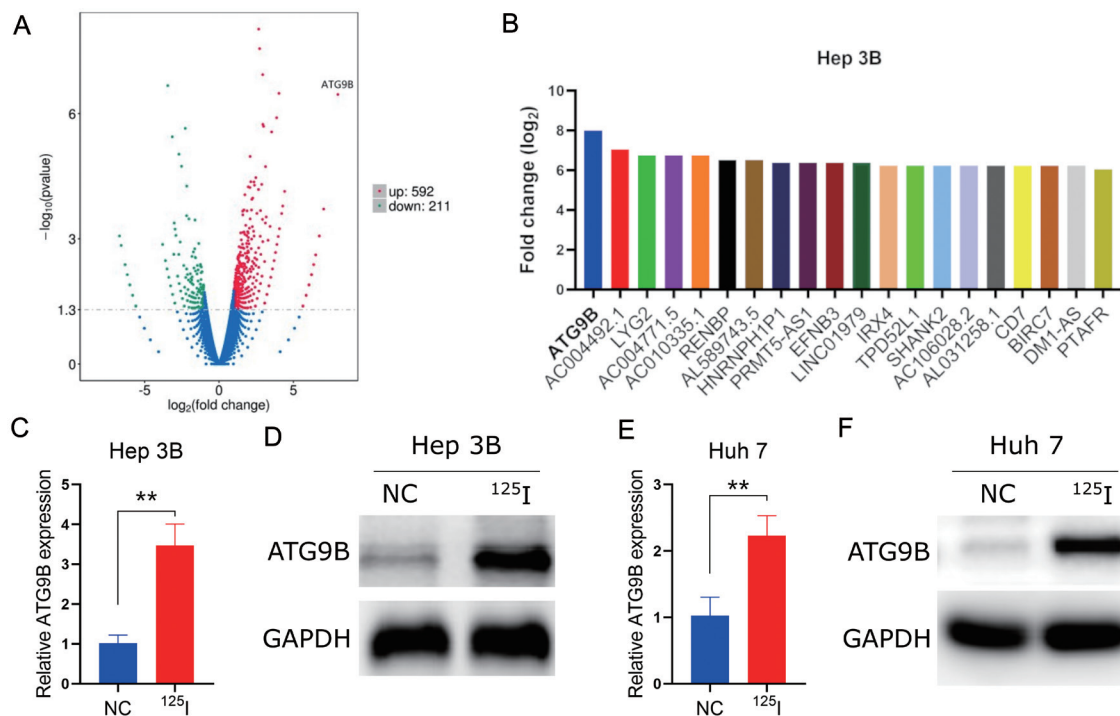


**Fig. 3.** <sup>125</sup>I particles increase ATG9B expression in HCC cells. (A) RNA sequencing analysis revealed 592 upregulated genes and 211 downregulated genes in Hep3B cells in the <sup>125</sup>I particle radiation group and control group. (B) The top 20 genes with significantly differentially increased expression from the RNA sequencing data. (C and E) The mRNA expression level of ATG9B in Hep3B and Huh7 cells treated with <sup>125</sup>I particle radiation for 72 h. GAPDH mRNA served as the internal reference. (D and F) Western blot analysis of ATG9B in Hep3B and Huh7 cells treated with <sup>125</sup>I particle radiation for 72 h. GAPDH was the internal reference. \*\**p*<0.01. HCC, hepatocellular carcinoma; ATG9B, autophagy-related 9B; <sup>125</sup>I, iodine-125; GAPDH, glyceraldehyde 3-phosphate dehydrogenase.

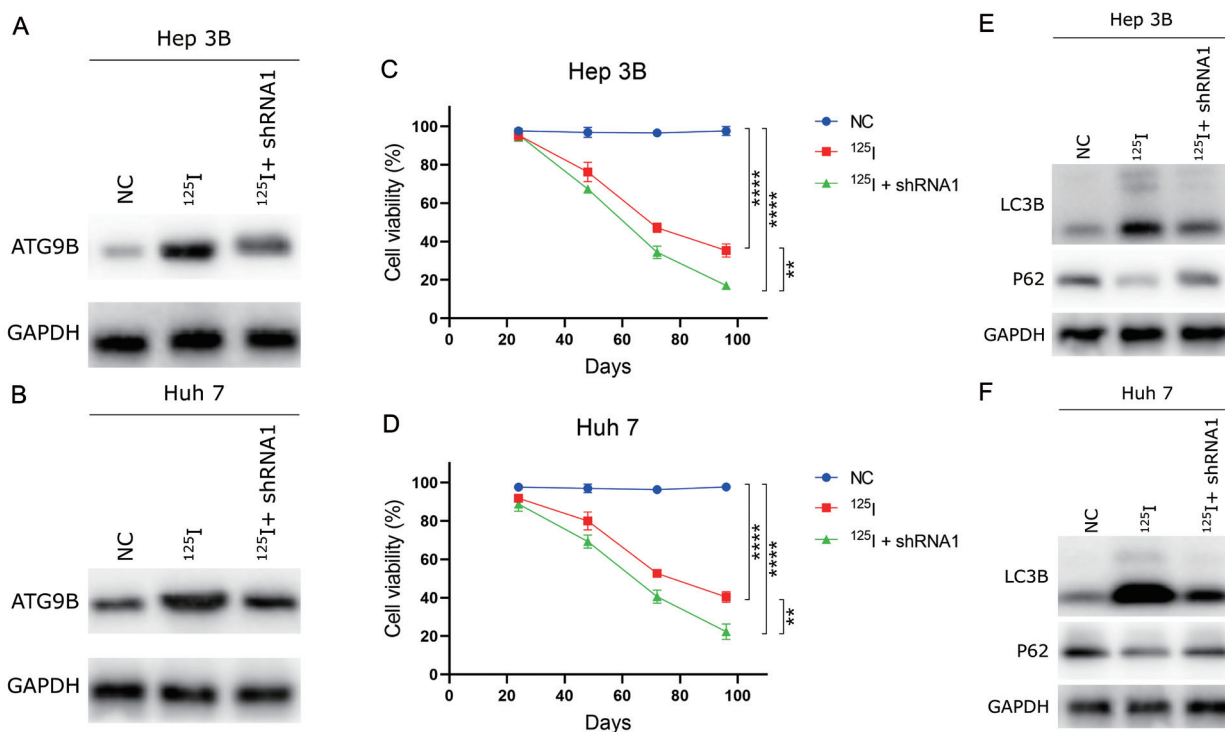


**Fig. 4.** <sup>125</sup>I particle radiation induces autophagy by increasing ATG9B *in vitro*. (A, B, E, F) Western blot analysis of ATG9B, LC3B, and p62 expression in ATG9B-silenced Hep3B and Huh7 cells with or without <sup>125</sup>I particle radiation. GAPDH served as the internal reference. (C, D) Cell viability was measured by a CCK-8 assay. \*\**p*<0.01, \*\*\*\**p*<0.0001. ATG9B, autophagy-related 9B; <sup>125</sup>I, iodine-125; GAPDH, glyceraldehyde 3-phosphate dehydrogenase.

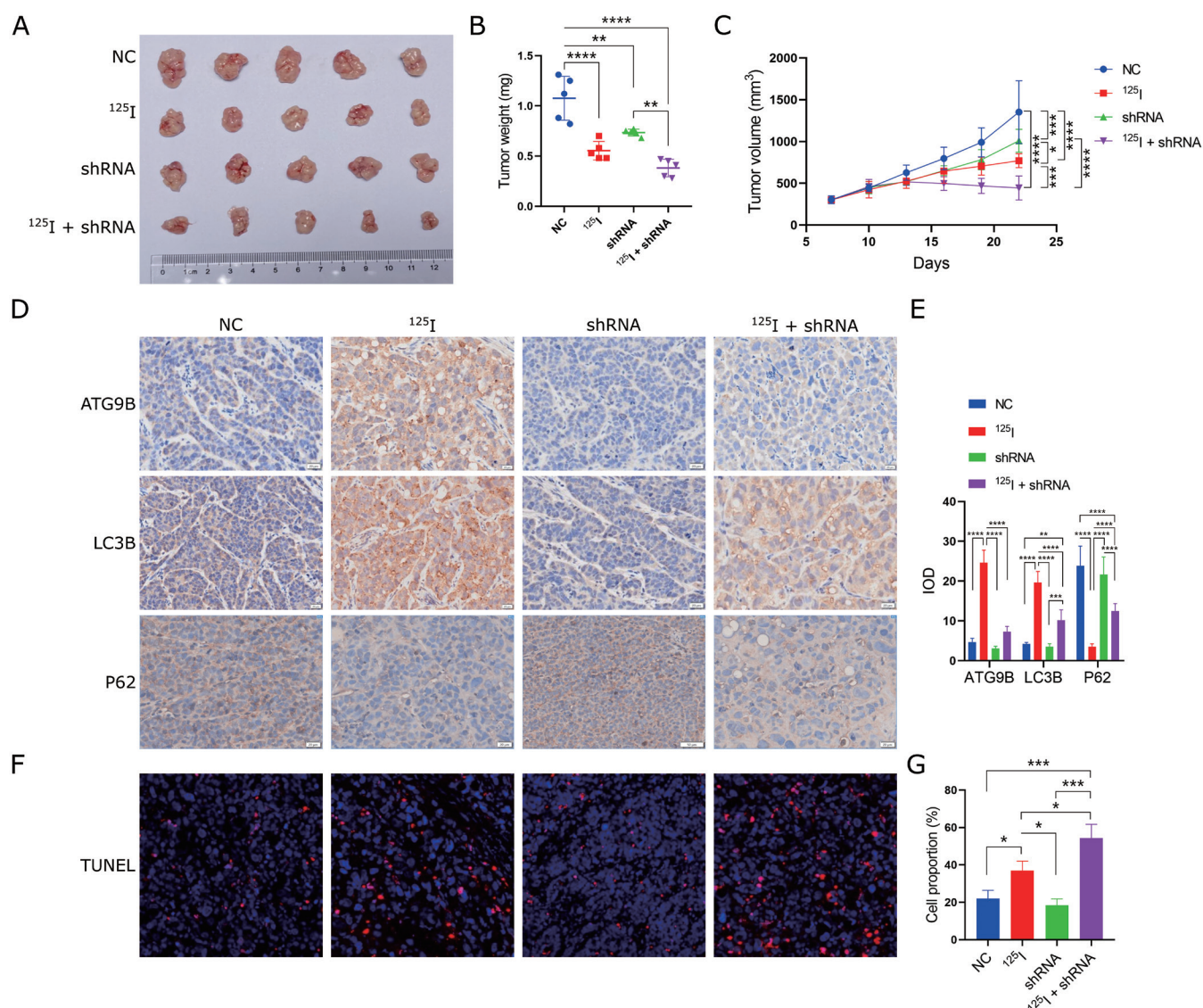


**Fig. 5.** <sup>125</sup>I particle radiation induces autophagy by increasing ATG9B *in vivo*. (A) Representative tumors with corresponding treatments. ATG9B silenced or negative control Hep3B cells were injected in nude mice, which were then divided into negative control, <sup>125</sup>I particle radiation, ATG9B shRNA and ATG9B shRNA + <sup>125</sup>I particle radiation groups and treated as described in "Materials and Methods" ( $n=5$  per group). (B) Tumor weight and (C) tumor volume of each group was measured at the end of the experiment. (D and E) Representative images of IHC staining of ATG9B, LC3B, and p62 in the xenografts (scale bar=20  $\mu$ m). (F and G) Representative images of TUNEL immunostaining for cell apoptosis in xenografts. \* $p<0.05$ , \*\* $p<0.01$ , \*\*\* $p<0.0001$ , \*\*\*\* $p<0.0001$ . <sup>125</sup>I, iodine-125; ATG9B, autophagy-related 9B; shRNA, short hairpin RNA; GAPDH, glyceraldehyde 3-phosphate dehydrogenase; IHC, immunohistochemical; TUNEL; terminal deoxynucleotidyl transferase dUTP nick end labeling.

with the dose, dose rate, and treatment volume.<sup>26</sup> Reducing the radioresistance of HCC patients and effectively killing tumor cells with the minimum dose of iodine-125 radioactive particles are of great significance for improving the effectiveness of radiotherapy and reducing the treatment cost borne by patients. In this study, we found that <sup>125</sup>I particle radiation mediated HCC cell apoptosis and autophagy *in vitro* and *in vivo* and we demonstrated that <sup>125</sup>I particle radiation-induced protective autophagy via regulating ATG9B expression in HCC cells using CQ. Moreover, silencing ATG9B enhanced the therapeutic effect of <sup>125</sup>I particle radiation on suppressing HCC proliferation, which may be a potential therapeutic strategy.

Autophagy, an evolutionarily conserved process, is the primary intracellular catabolic mechanism that responds to both intracellular and extracellular stress (e.g. cytoplasmic com-

ponents, pathogenic infection, radiation damage, nutrient starvation, hypoxia), and involves lysosomal degradation and recycling of unnecessary or dysfunctional components.<sup>27</sup> The functioning of autophagy in liver cancer is a topic of concern. Autophagy has multiple roles in different situations. In normal liver cells, basal autophagy has a housekeeping function in maintaining liver homeostasis, and it also prevents tumorigenesis by removing harmful mitochondria. After HCC has developed, autophagy promotes tumor development, metastasis, and therapeutic resistance.<sup>24,28</sup> With limited activation, autophagy removes cells with radiation-induced injury and promotes cell survival, thus inducing radiation resistance; this function has been well established in numerous cancers such as glioma and lung, breast, and pancreatic cancer.<sup>29-32</sup> With continuous activation, damaged cellular organelles and metabolites are degraded, resulting in autophagy-related cell

death or apoptosis.<sup>33</sup> In general, radiation tends to induce cytoprotective autophagy. Notably, whether HCC is resistant to <sup>125</sup>I particle radiation remains unclear. Our findings demonstrate that <sup>125</sup>I particles not only induced HCC cell death but also stimulated autophagy. We further found that <sup>125</sup>I particle mediated protective autophagy as shown by the observation that the autophagy inhibitor CQ enhanced the toxicity of <sup>125</sup>I particles on HCC cells. In addition, experiments using a xenograft mouse model provided *in vivo* evidence that CQ enhanced the radiation sensitivity of Hep3B xenografts. Our results suggested that <sup>125</sup>I particles combined with CQ may be a good therapeutic strategy for HCC. This strategy has achieved similar results in esophageal cancer and bladder cancer.<sup>34,35</sup>

Transcriptome sequencing is effective for identifying functional molecular and molecular signaling pathways.<sup>36–39</sup> Using transcriptome sequencing and bioinformatics analysis, we found that <sup>125</sup>I particle radiation increased the expression of hundreds of genes, and that *ATG9B* expression was the most upregulated. *ATG9B* is a key protein in autophagosome formation and autophagy initiation in mammalian cells.<sup>40</sup> LC3 is used to monitor to autophagic activity and is related to autophagosome development and maturation.<sup>41</sup> *ATG9B*-driven phagophores might activate docking of both LC3 and p62 and further initiate autophagy-associated degradation.<sup>42</sup> Once *ATG9B* is inhibited, LC3 lipidation and autophagic punctuations are subsequently reduced.<sup>42</sup> In this study, silencing of *ATG9B* inhibited <sup>125</sup>I particle radiation-mediated protective autophagy in HCC cells, suggesting that *ATG9B* participates in the autophagy process at a critical step. Furthermore, silencing *ATG9B* inhibited tumor growth and enhanced <sup>125</sup>I particle radiation sensitivity in HCC *in vivo*. Our results indicate that <sup>125</sup>I particles combined with an *ATG9B* inhibitor might be beneficial for HCC therapy. In addition, we did not detect a significant change of *ATG9A* expression in HCC cells with or without <sup>125</sup>I particle radiation, so we did not explore its activity in HCC cells. Whether *ATG9A* has biological functions in <sup>125</sup>I particle radiation-mediated HCC cell death needs to be further explored.

## Conclusions

<sup>125</sup>I particle radiation-induced protective autophagy by increasing *ATG9B* expression in HCC cells. *ATG9B* inhibition combined with <sup>125</sup>I particle radiation enhanced the effectiveness of <sup>125</sup>I particle radiation to suppress the growth of HCC. Our findings suggest that <sup>125</sup>I particle radiation plus CQ or/and an *ATG9B* inhibitor may be a novel therapeutic strategy for HCC.

## Acknowledgments

The authors sincerely thank Mr. Bosheng Li for his technical support during the experiments.

## Funding

This study was supported by the Science and Technology Innovation Project of Social Undertakings and Livelihood Security in Chongqing (No. cstc2016shms-ztx0045).

## Conflict of interest

The authors have no conflict of interests related to this publication.

## Author contributions

Design and supervision of the experiments, and revision of the manuscript (FH, XH), performance of the experiments (YX, JY, CY, JX, LD, QL, CH, LL), writing of the first draft of the manuscript (YX, JY), analysis of the data and revision of the manuscript (QL, CH, LL). All authors have seen and approved the final version of this paper.

## Ethical statement

All animal experiments were conducted in accordance with the guidelines of animal care and were reviewed and approved by the ethics committee of the First Affiliated Hospital of Army Medical University (No. AMUWEC20200407).

## Data sharing statement

The datasets generated and analyzed during the current study are not publicly available due to none of the data types requiring uploading to a public repository but are available from the corresponding author on reasonable request.

## References

- [1] Siegel RL, Miller KD, Jemal A. Cancer statistics, 2020. *CA Cancer J Clin* 2020;70(1):7–30. doi:10.3322/caac.21590, PMID:31912902.
- [2] Sung H, Ferlay J, Siegel RL, Laversanne M, Soerjomataram I, Jemal A, *et al*. Global Cancer Statistics 2020: GLOBOCAN Estimates of Incidence and Mortality Worldwide for 36 Cancers in 185 Countries. *CA Cancer J Clin* 2021;71(3):209–249. doi:10.3322/caac.21660, PMID:33538338.
- [3] European Association for the Study of the Liver. EASL Clinical Practice Guidelines: Management of hepatocellular carcinoma. *J Hepatol* 2018;69(1):182–236. doi:10.1016/j.jhep.2018.03.019, PMID:29628281.
- [4] Song Z, Ye J, Wang Y, Li Y, Wang W. Computed tomography-guided iodine-125 brachytherapy for unresectable hepatocellular carcinoma. *J Cancer Res Ther* 2019;15(7):1553–1560. doi:10.4103/jcrt.JCRT\_629\_19, PMID:31939437.
- [5] Wang W, Wang C, Shen J, Ren B, Yin Y, Yang J, *et al*. Integrated I-125 Seed Implantation Combined with Transarterial Chemoembolization for Treatment of Hepatocellular Carcinoma with Main Portal Vein Tumor Thrombus. *Cardiovasc Intervent Radiol* 2021;44(10):1570–1578. doi:10.1007/s00270-021-02887-1, PMID:34117503.
- [6] Zhu ZX, Wang XX, Yuan KF, Huang JW, Zeng Y. Transarterial chemoembolization plus iodine-125 implantation for hepatocellular carcinoma: a systematic review and meta-analysis. *HPB (Oxford)* 2018;20(9):795–802. doi:10.1016/j.hpb.2018.03.015, PMID:29779970.
- [7] Li F, Xu J, Zhu Y, Sun L, Zhou R. Analysis of Cells Proliferation and MicroRNAs Expression Profile in Human Chondrosarcoma SW1353 Cells Exposed to Iodine-125 Seeds Irradiation. *Dose Response* 2020;18(2):1559325820920525. doi:10.1177/1559325820920525, PMID:32362797.
- [8] Zhu HD, Guo JH, Huang M, Ji JS, Xu H, Lu J, *et al*. Irradiation stents vs. conventional metal stents for unresectable malignant biliary obstruction: A multicenter trial. *J Hepatol* 2018;68(5):970–977. doi:10.1016/j.jhep.2017.12.028, PMID:29331343.
- [9] Zhang F, Wang J, Guo J, Li Y, Huang X, Guan Z, *et al*. Chinese Expert Consensus Workshop Report: Guideline for permanent iodine-125 seed implantation of primary and metastatic lung tumors. *Thorac Cancer* 2019;10(2):388–394. doi:10.1111/1759-7714.12912, PMID:30521144.
- [10] Ohri N, Dawson LA, Krishnan S, Seong J, Cheng JC, Sarin SK, *et al*. Radiotherapy for Hepatocellular Carcinoma: New Indications and Directions for Future Study. *J Natl Cancer Inst* 2016;108(9):djw133. doi:10.1093/jnci/djw133, PMID:27377923.
- [11] Amaravadi RK, Kimmelman AC, Debnath J. Targeting Autophagy in Cancer: Recent Advances and Future Directions. *Cancer Discov* 2019;9(9):1167–1181. doi:10.1158/2159-8290.cd-19-0292, PMID:31434711.
- [12] Yang S, Yang L, Li X, Li B, Li Y, Zhang X, *et al*. New insights into autophagy in hepatocellular carcinoma: mechanisms and therapeutic strategies. *Am J Cancer Res* 2019;9(7):1329–1353. PMID:31392073.
- [13] Tam SY, Wu VW, Law HK. Influence of autophagy on the efficacy of radiotherapy. *Radiat Oncol* 2017;12(1):57. doi:10.1186/s13014-017-0795-y, PMID:28320471.
- [14] Li X, He S, Ma B. Autophagy and autophagy-related proteins in cancer. *Mol Cancer* 2020;19(1):12. doi:10.1186/s12943-020-1138-4, PMID:31969156.
- [15] Denton D, Kumar S. Autophagy-dependent cell death. *Cell Death Differ* 2019;26(4):605–616. doi:10.1038/s41418-018-0252-y, PMID:30568239.

- [16] Long M, McWilliams TG. Monitoring autophagy in cancer: From bench to bedside. *Semin Cancer Biol* 2020;66:12–21. doi:10.1016/j.semcancer.2019.05.016, PMID:31319163.
- [17] Hu L, Wang H, Huang L, Zhao Y, Wang J. The Protective Roles of ROS-Mediated Mitophagy on (125I) Seeds Radiation Induced Cell Death in HCT116 Cells. *Oxid Med Cell Longev* 2016;2016:9460462. doi:10.1155/2016/9460462, PMID:28119765.
- [18] Wang C, Li TK, Zeng CH, Fan R, Wang Y, Zhu GY, et al. Iodine-125 seed radiation induces ROS-mediated apoptosis, autophagy and paraptosis in human esophageal squamous cell carcinoma cells. *Oncol Rep* 2020;43(6):2028–2044. doi:10.3892/or.2020.7576, PMID:32323828.
- [19] Vigneault E, Martell K, Taussky D, Husain S, Delouya G, Mbodji K, et al. Does Seed Migration Increase the Risk of Second Malignancies in Prostate Cancer Patients Treated With Iodine-125 Loose Seeds Brachytherapy? *Int J Radiat Oncol Biol Phys* 2018;100(5):1190–1194. doi:10.1016/j.ijrobp.2017.12.273, PMID:29428250.
- [20] Ji Z, Jiang Y, Tian S, Guo F, Peng R, Xu F, et al. The Effectiveness and Prognostic Factors of CT-Guided Radioactive I-125 Seed Implantation for the Treatment of Recurrent Head and Neck Cancer After External Beam Radiation Therapy. *Int J Radiat Oncol Biol Phys* 2019;103(3):638–645. doi:10.1016/j.ijrobp.2018.10.034, PMID:30391521.
- [21] Jia SN, Wen FX, Gong TT, Li X, Wang HJ, Sun YM, et al. A review on the efficacy and safety of iodine-125 seed implantation in unresectable pancreatic cancers. *Int J Radiat Biol* 2020;96(3):383–389. doi:10.1080/09553002.2020.1704300, PMID:31977258.
- [22] Lin ZY, Chen J, Deng XF. Treatment of hepatocellular carcinoma adjacent to large blood vessels using 1.5T MRI-guided percutaneous radiofrequency ablation combined with iodine-125 radioactive seed implantation. *Eur J Radiol* 2012;81(11):3079–3083. doi:10.1016/j.ejrad.2012.05.007, PMID:22673775.
- [23] Li D, Wang WJ, Wang YZ, Wang YB, Li YL. Lobaplatin promotes (125I)-induced apoptosis and inhibition of proliferation in hepatocellular carcinoma by upregulating PERK-eIF2 $\alpha$ -ATF4-CHOP pathway. *Cell Death Dis* 2019;10(10):744. doi:10.1038/s41419-019-1918-1, PMID:31582720.
- [24] Huang F, Wang BR, Wang YG. Role of autophagy in tumorigenesis, metastasis, targeted therapy and drug resistance of hepatocellular carcinoma. *World J Gastroenterol* 2018;24(41):4643–4651. doi:10.3748/wjg.v24.i41.4643, PMID:30416312.
- [25] Zhang FJ, Li CX, Zhang L, Wu PH, Jiao DC, Duan GF. Short- to mid-term evaluation of CT-guided 125I brachytherapy on intra-hepatic recurrent tumors and/or extra-hepatic metastases after liver transplantation for hepatocellular carcinoma. *Cancer Biol Ther* 2009;8(7):585–590. doi:10.4161/cbt.8.7.7902, PMID:19276683.
- [26] Escande A, Haie-Meder C, Mazeron R, Maroun P, Cavalcanti A, de Crevoisier R, et al. Brachytherapy for Conservative Treatment of Invasive Penile Carcinoma: Prognostic Factors and Long-Term Analysis of Outcome. *Int J Radiat Oncol Biol Phys* 2017;99(3):563–570. doi:10.1016/j.ijrobp.2017.02.090, PMID:28501419.
- [27] Levine B, Klionsky DJ. Development by self-digestion: molecular mechanisms and biological functions of autophagy. *Dev Cell* 2004;6(4):463–477. doi:10.1016/s1534-5807(04)00099-1, PMID:15068787.
- [28] Wang N, Tan HY, Li S, Feng Y. Atg9b Deficiency Suppresses Autophagy and Potentiates Endoplasmic Reticulum Stress-Associated Hepatocyte Apoptosis in Hepatocarcinogenesis. *Theranostics* 2017;7(8):2325–2338. doi:10.7150/thno.18225, PMID:28740555.
- [29] Chaachouay H, Ohneseit P, Toulany M, Kehlbach R, Multhoff G, Rodemann HP. Autophagy contributes to resistance of tumor cells to ionizing radiation. *Radiother Oncol* 2011;99(3):287–292. doi:10.1016/j.radonc.2011.06.002, PMID:21722986.
- [30] Yao KC, Komata T, Kondo Y, Kanzawa T, Kondo S, Germano IM. Molecular response of human glioblastoma multiforme cells to ionizing radiation: cell cycle arrest, modulation of the expression of cyclin-dependent kinase inhibitors, and autophagy. *J Neurosurg* 2003;98(2):378–384. doi:10.3171/jns.2003.98.2.0378, PMID:12593626.
- [31] Wang P, Zhang J, Zhang L, Zhu Z, Fan J, Chen L, et al. MicroRNA 23b regulates autophagy associated with radioresistance of pancreatic cancer cells. *Gastroenterology* 2013;145(5):1133–1143.e1112. doi:10.1053/j.gastro.2013.07.048, PMID:23916944.
- [32] Koukourakis MI, Mitrakas AG, Giromanolaki A. Therapeutic interactions of autophagy with radiation and temozolomide in glioblastoma: evidence and issues to resolve. *Br J Cancer* 2016;114(5):485–496. doi:10.1038/bjc.2016.19, PMID:26889975.
- [33] Zhang X, Wang J, Li X, Wang D. Lysosomes contribute to radioresistance in cancer. *Cancer Lett* 2018;439:39–46. doi:10.1016/j.canlet.2018.08.029, PMID:30217567.
- [34] Wang C, Li TK, Zeng CH, Yang J, Wang Y, Lu J, et al. Inhibition of Endoplasmic Reticulum Stress-Mediated Autophagy Enhances the Anticancer Effect of Iodine-125 Seed Radiation on Esophageal Squamous Cell Carcinoma. *Radiat Res* 2020;194(3):236–245. doi:10.1667/rade-20-00057.1, PMID:32942301.
- [35] Wang F, Tang J, Li P, Si S, Yu H, Yang X, et al. Chloroquine Enhances the Radiosensitivity of Bladder Cancer Cells by Inhibiting Autophagy and Activating Apoptosis. *Cell Physiol Biochem* 2018;45(1):54–66. doi:10.1159/000486222, PMID:29316551.
- [36] Farkas MH, Au ED, Sousa ME, Pierce EA. RNA-Seq: Improving Our Understanding of Retinal Biology and Disease. *Cold Spring Harb Perspect Med* 2015;5(9):a017152. doi:10.1101/cshperspect.a017152, PMID:25722474.
- [37] Byron SA, Van Keuren-Jensen KR, Engelthaler DM, Carpten JD, Craig DW. Translating RNA sequencing into clinical diagnostics: opportunities and challenges. *Nat Rev Genet* 2016;17(5):257–271. doi:10.1038/nrg.2016.10, PMID:26996076.
- [38] Wang Z, Gerstein M, Snyder M. RNA-Seq: a revolutionary tool for transcriptomics. *Nat Rev Genet* 2009;10(1):57–63. doi:10.1038/nrg2484, PMID:19015660.
- [39] Maher CA, Kumar-Sinha C, Cao X, Kalyana-Sundaram S, Han B, Jing X, et al. Transcriptome sequencing to detect gene fusions in cancer. *Nature* 2009;458(7234):97–101. doi:10.1038/nature07638, PMID:19136943.
- [40] He C, Baba M, Cao Y, Klionsky DJ. Self-interaction is critical for Atg9 transport and function at the phagophore assembly site during autophagy. *Mol Cell* 2008;19(12):5506–5516. doi:10.1091/mbc.e08-05-0544, PMID:18829864.
- [41] Schaaf MB, Keulers TG, Vooijs MA, Rouschop KM. LC3/GABARAP family proteins: autophagy-(un)related functions. *Faseb j* 2016;30(12):3961–3978. doi:10.1096/fj.201600698R, PMID:27601442.
- [42] Chen D, Chen X, Li M, Zhang H, Ding WX, Yin XM. CCCP-Induced LC3 lipidation depends on Atg9 whereas FIP200/Atg13 and Beclin 1/Atg14 are dispensable. *Biochem Biophys Res Commun* 2013;432(2):226–230. doi:10.1016/j.bbrc.2013.02.010, PMID:23402761.